INVESTIGATING CARBON DYNAMICS OF A YOUNG TEMPERATE CONIFEROUS FOREST USING LONG-TERM EDDY COVARIANCE FLUX OBSERVATIONS

INVESTIGATING CARBON DYNAMICS OF A YOUNG TEMPERATE CONIFEROUS FOREST USING LONG-TERM EDDY COVARIANCE FLUX OBSERVATIONS

By
Farbod Tabaei, B.Sc.

A Thesis Submitted to the School of Graduate Studies
In Partial Fulfillment of the Requirements
For the Degree Master of Science

McMaster University © Copyright by Farbod Tabaei, April 2023

McMaster University
Master of Science (2023)
Earth, Environment & Society
Hamilton, Ontario, Canada

TITLE: Investigating Carbon Dynamics of a Young Temperate Coniferous Forest Using Long-Term Eddy Covariance Flux Observations

AUTHOR: Farbod Tabaei, B.Sc. [Env Sci] (McMaster University)

SUPERVISOR: Dr. M. Altaf Arain

NUMBER OF PAGES: x, 45

ABSTRACT

Plantation and managed forests are major sink of atmospheric CO_2 in North America and across the world. If properly managed, these forests may help to offset anthropogenic greenhouse gas emissions to mitigate climate change. This study investigated the impacts of climate variability, extreme weather events, and disturbance (thinning) on the growth and carbon (C) exchanges of a young temperate coniferous plantation forest (48-year-old white pine (Pinus strobus)) in the Great Lakes region in Canada using long-term eddy covariance flux observations. CO_2 fluxes, as well as meteorological and soil variables were continuously measured from 2008 to 2021 (14 years) to estimate net ecosystem productivity (NEP), ecosystem respiration (RE), and gross ecosystem productivity (GEP). Soil respiration (Rs) was also measured using automatic soil chambers from 2017 to 2019. Selective thinning was conducted first time in this stand in January 2021 to remove approximately 1/3 of the basal area. Study results showed that climate conditions in the early growing season, from late May to mid-July, determined the overall strength of C uptake in any given year. However, above-average temperature and precipitation in the late growing season significantly reduced NEP and even in some cases, transformed the forest into a net C source for short periods due to large pulses of RE. Mean annual GEP, RE and NEP values were 1660 ±199, 1087 ±96 and 592 ±169 g C m^{-2} yr^{-1}, respectively, from 2008 to 2021. Thinning did not significantly impact the C uptake of the forest as the stand remained a net C sink with an annual NEP of 648 g C m^{-2} yr^{-1} in 2021. Changes in annual GEP, RE and NEP in 2021 remained within the range of interannual variability over the study period. Overall, Rs accounted for roughly 89% of the annual RE in this stand. A complete understanding of the response of forest C dynamics to climate variability and thinning in young plantation forests is critical to guiding future forest management efforts for enhancing the growth and C uptake of these forest plantations to maximize their potential in support of providing nature-based climate solutions.

ACKNOWLEDGEMENTS

First and foremost, I would like to thank my mentor and supervisor, Dr. Altaf Arain for his guidance and support during my time as a MSc student. He provided me with many great opportunities and invaluable advice, allowing me to further push my boundaries and capabilities in the field of research. I will be forever thankful for the lifelong skills I have gained under his supervision and support. I would also like to express my gratitude to the members of my supervisory committee: Dr. Sean Carey and Dr. Mike Waddington.

I would also like to extend my wholehearted appreciation to my colleagues in the Climate Centre and lab for their camaraderie and all the memories we made along the way. It is an honour for me to have been a part of such talented and smart group of researchers: Jason Brodeur, Tariq Deen, Nur Hussain, Lejla Latifovic, Daniel Mutton, Elizabeth Arango Ruda, and Noah Stegman.

I am truly grateful to my amazing family and partner for their unconditional and everlasting love and support. They have been my biggest source of encouragement and I will be forever indebted to the sacrifices they have made for me to be in this position.

This study was funded by the Natural Sciences and Engineering Research Council (NSREC), the Global Water Futures Program (GWF), and the Ontario Ministry of Environment and Climate Change (MOECC). Support from the Ontario Ministry of Natural Resources and Forestry (OMNRF) and the St. Williams Conservation Reserve Community Council (SWCRCC) is also acknowledged.

TABLE OF CONTENTS

LIST OF FIGURES

LIST OF TABLES

SYMBOLS AND ABBREVIATIONS

θ	volumetric water content	($m^3\ m^{-3}$)
ΔS	CO_2 storage change below sensors	
C	carbon	
CO_2	carbon dioxide	
DBH	diameter at breast height	(cm)
EC	eddy covariance	
FCRN	Fluxnet Canada Research Network	
GEP	gross ecosystem productivity	(g C m^{-2})
RE	ecosystem respiration	(g C m^{-2})
IRGA	infrared gas analyzer	
LAI	leaf area index	($m^3\ m^{-3}$)
NEE	net ecosystem exchange	(g C m^{-2})
NEP	net ecosystem productivity	(g C m^{-2})
NFI	Canadian National Forestry Inventory	
PAR	photosynthetic active radiation	(μmol $m^{-2}\ s^{-1}$)
PPT	precipitation	(mm)
REW	relative extractable water	
REW_{min}	daily minimum relative extractable water	
RH	relative humidity	(%)
Rh	heterotrophic respiration	(g C m^{-2})
Rs	soil respiration	(g C m^{-2})
Ta	air temperature above canopy	(°C)
T_{max}	daily maximum air temperature above canopy	(°C)
TP39	83-year-old white pine plantation	
TP74	48-year-old white pine plantation	
Ts	soil temperature	(°C)
u_*	friction velocity	
u_*^{Th}	friction velocity threshold	
VPD	vapour pressure deficit	(kPa)
WUE	water use efficiency	

CHAPTER 1: INTRODUCTION

1.1. Background

Forests play a critical role in the global carbon cycle by storing large amounts of carbon (C). Forests sequester atmospheric CO_2 through photosynthesis and store it in various tree components or live pools. Other biological processes, such as litterfall and tree mortality, eventually move a considerable fraction of this C to forest soil. Around 234 Pg of C is estimated to be stored aboveground in the forests, 398 Pg C in forest soils, 41 Pg C in deadwood and 23 Pg C in litter pools (Kindermann et al., 2008). The expansion of agricultural land was the primary driver of deforestation in temperate regions in eastern North America in the early 19th century. This was followed by the large-scale abandonment of these agricultural fields by the mid-20th century due to urbanization and industrial development (Richart & Hewitt, 2008). Abandoned agricultural lands in eastern North America offer an opportunity to contribute to nature-based climate solutions by establishing plantation forests and enhancing their C sequestration capabilities through developing climate-adapted management practices (Arain et al., 2022).

Thinning – harvesting a specific portion of trees is a common silviculture or forest management practice to sustain and improve the growth and productivity of forests (Ashton & Kelty, 2018). Thinning reduces resource competition among the remaining trees by lowering the demand for water, light and nutrients while providing economic benefits through higher yields of harvested timber. Reduction of canopy coverage due to tree removal has also been shown to impact forest biodiversity by promoting the growth

of lower canopy, with such impact being more pronounced in closed canopy forests prior to thinning (Wilson & Puettmann, 2007). Recent studies have indicated enhanced drought resilience, reduced tree mortality, and increased water use efficiency (WUE) following thinning, which can be of great use in the face of climate change and increasing drought intensity and frequency (Bodo & Arain, 2021; Knapp et al., 2021; Skubel et al., 2017).

Eastern white pine (*Pinus strobus*) is a native tree species in eastern North America which is highly adaptable to a wide range of environments and soil conditions. It is a preferred tree species to establish plantation stands. White pine has also been observed to grow naturally in abandoned or disturbed agricultural lands. Disturbed and eroded soils can favour the growth and early establishment of white pine seedlings due to the low risk of disease and competing vegetation (Ostry et al., 2010). Furthermore, young white pine plantation forests have been found to be a large C sink due to their rapid growth and establishment. Previous studies have demonstrated that net ecosystem productivity (NEP) in these plantation stands peaks about three decades earlier than naturally regenerated forests that generally peak at about 50 to 70 years of age (Arain et al., 2022; Peichl et al., 2010). Despite about 3% decrease in total global forested area between 1990 and 2015, area of new plantation forests increased globally from 167.5 million ha to 277.9 million ha during the same period, where 56% of these plantations were established in temperate regions (Payn et al., 2015). While these newly established forests are considered a major sink of C due to high productivity, there is lack of literature studies and adequate long-term CO_2 flux data to fully understand the response of these young forests to climate

change and extreme weather events (Chan et al., 2018; Xu et al., 2020). A complete understanding of climate change, extreme weather and management (thinning) impacts on young plantation forests is essential to fully realize their potential for C sequestration to offset atmospheric greenhouse gas emissions.

1.2. Objectives and hypothesis

In this study, we examine the impacts of climate variability and selective thinning that was conducted in this closed-canopy plantation forest to remove approximately 1/3 of basal area in January 2021. The objectives are to (i) explore the impacts of climate variability and extreme weather events (e.g. heat and drought stress) on the gross ecosystem productivity (GEP), ecosystem respiration (RE) and net ecosystem productivity (NEP) using EC flux data from 2008 to 2021 and (ii) determine how disturbance (thinning) might have influenced the magnitude and direction of these C fluxes. We hypothesize an insignificant impact on GEP following the first post-thinning year, with increase in RE being the dominant factor in carbon fluxes of the plantation.

1.3. Study significance

Our study is among handful of global flux tower sites exploring carbon flux dynamic of a middle age (48-year old) planation forest in Southern Ontario, Canada, which is at the peak of its C uptake life cycle and where long-term (14 years) eddy covariance (EC) flux data is available. Long-term continuous observation of C fluxes, soil respiration and meteorological variables provide valuable insight into the temporal dynamics of forests

and their response to climate change and extreme weather events, allowing the researchers to detect and analyze patterns and trends that would be hard to detect in short-term studies. This information is crucial for developing effective climate change adaptation and resilience strategies for forest ecosystems.

CHAPTER 2: METHODOLOGY

2.1. Study site

This study was conducted in a 48-year-old temperate coniferous forest (42.707364°N, 80.348524°W), one of the five Turkey Point Environmental Observatory (TPEO) flux tower stations located north of Lake Erie southern Ontario, Canada (Arain 2018a; Arain et al., 2022). The study site is referred to as CA-TP3 in Ameriflux or TP74 in some other publications with 1974 representing the year it was planted. This site is owned by the Ontario Ministry of Natural Resources and Forestry and is part of St. Williams Conservation Reserve -Turkey Point Tract. The forest is considered a monoculture stand with predominant species of Pinus strobus (Eastern white pine) and infrequent numbers of Pinus sylvestris (Scotch pine) and Pinus resinosa (Red pine). Scattered regeneration of Quercus velutina (Black oak), Fraxinus americana (White ash), and advanced (2-5 meters) Acer rubrum (Red maple) has been observed throughout the site. The plantation was carried out on previously cleared oak savannah for the purpose of stabilization of the eroding sandy soil and timber production.

The soil of the study site is well-drained with low to moderate water-holding capacity and is categorized by the Canadian Soil Classification Scheme as Brunisolic Gray Brown Luvisol. Measurements indicate high composition of sand (~98% sand, 1% silt, <1% clay), bulk density of 1.376 (g cm^{-3}), and water table at a depth of 6-7 m. The volumetric water content at wilting point and field capacity is estimated to be 0.01 m^3 m^{-3} and 0.2 m^3 m^{-3}, respectively (Arain et al., 2022). A summary of site characteristics is provided in Table 1.

The Climate in the region is humid continental exhibiting warm summers and cool winters. The 30-year (1981-2010) average air temperature and total precipitation are 8.0 °C and 1036 mm, respectively, based on Environment Canada measurements from a weather station at Delhi, Ontario, approximately 20 km northwest of the site. Precipitation is evenly distributed throughout the year, and 14% falls as snow.

2.2. Thinning operation

In the winter (January) of 2021, a partial thinning was conducted in the forest where every 4^{th} row, plus a few trees from either side of the row were removed by machine harvesting with the aim of overall removal of about a third of the basal area, with a focus on smaller poor-quality conifers. The new-growth hardwood species were preserved, and the surrounding vegetation was removed to enhance their productivity and survival rate. Only logs were removed, and residual live/dead branches and foliage were left on the ground after harvesting. The site's pre- and post-thinning values of the basal area are

estimated to be 35 m^2/ha and 22 m^2/ha, respectively. Partial thinning removed approximately 63 m^3/ha of wood volume.

2.3. Eddy covariance flux and meteorological measurements

Half-hourly CO_2, energy and water fluxes were continuously measured on top of a 20m high walk-up scaffolding tower from January 2008 to December 2021 using a closed-path eddy covariance (EC) technique and following Fluxnet Canada Research Network (FCRN) protocols. The closed-path EC system comprised a 3-D sonic anemometer (model CSAT-3, Campbell Scientific Inc.), an infrared gas analyzer (IRGA, model LI-7000, LI-COR Inc.) and a climate control box with heated tubing. Fluxes were measured at 20 Hz and then sampled to half-hourly values. The EC data were stored on a desktop computer in a nearby hut. The site is equipped with AC power and internet connection. Calibration of IRGA was conducted on a monthly basis using high-purity nitrogen and standardized CO_2 gases to set the zero and span offset. The CO_2 storage change (ΔS) in the air column below the EC sensors was estimated using CO_2 concentration measurements made at the top of the tower by the EC system and an IRGA (model LI-800 LI-COR Inc.) that sampled it from mid-canopy. The net ecosystem exchange (NEE) was calculated as $NEE = Fc + \Delta S$. NEP calculations are the inverse of NEE (NEP = -NEE), with positive NEP values indicating a net carbon sink and negative values a carbon source for the forest.

Meteorological variables for the study period were also measured alongside EC calculations for air temperature (Ta) and relative humidity (RH, model HMP45C, Campbell Scientific Inc.), net radiation (model NR-LITE, Kipp and Zonen Ltd), downward and upward photosynthetically active radiation (PAR, model LI-200S, LI-COR Inc.), wind speed and wind direction (model 05103-10, R.M. Young Co.) and atmospheric pressure (model 61,205 V, R.M. Young Co.). Precipitation (PPT) was measured near the site in an open area using a weighted accumulation rain gauge (model T200B, Geonor Inc.). Soil temperature (model 107, Campbell Scientific Inc.) was measured at 2, 5, 10, 20, 50 and 100 cm depths, while soil moisture (model CS615, Campbell Scientific Inc.) was measured at 5, 10, 20, 50 and 100 cm depths at two locations near the tower. All meteorological variables were sampled at 5 seconds and averaged at half-hourly intervals.

2.4. Soil respiration flux measurements

Soil CO_2 efflux or soil respiration (Rs) was measured at half-hourly intervals using an automated chamber system (model 8100-104, LI-COR Inc.) comprising a gas analyzer control unit (LI-8100A, LI-COR Inc.) and a multiplexer (LI-8150, LI-COR Inc.) for simultaneous measurement of multiple (3 to 5) chambers. Measurements were conducted in the snow-free growing seasons from 2017 to 2019, with the chambers placed on top of permanent collars to reduce soil disturbance. The PVC collars have a thickness of 1 cm, a 20 cm diameter, and a height of 11.4 cm, with at least 2 cm extending above the soil. During the measurement period, any vegetation growing in the collars was removed to

eliminate the effects of photosynthesis on Rs calculations. The chambers were located approximately 15 m from the control unit, housed in the EC system hut near the tower. The automatic soil chamber system estimates Rs by measuring the rate of increase in CO_2 concentration during chamber closure over 3 minutes and fitting a nonlinear equation (Healy et al., 1996).

2.5. Gap-filling and data processing

Quality control of all C flux and meteorological data was conducted using the Biometeorological Analysis, Collection, and Organizational Node (BACON) software based on the Flxnet Canada and AmeriFlux network protocols, following Brodeur (2014). Smaller meteorological gaps up to a few hours were filled using linear interpolation, while larger gaps were filled with data from other nearby TPFS sites such as CA-TP4 (Arain 2018b; Arain et al., 2022)

Periods of low turbulence with minimal vertical air movement (mostly at nighttime) can lead to underestimation of EC measurements. Friction velocity (u_*) is a measure of the degree of turbulent mixing with lower values indicating a stable atmosphere and low vertical turbulence. To remove underestimated data, a site-specific friction-velocity threshold (u_*^{Th}) of 0.5 was applied to remove nighttime (PAR < 100 μmol m^{-2} s^{-1}) NEP values below the threshold (Barr et al., 2013; Papale et al., 2006). A three-dimensional Lagrangian footprint model was used to calculate half-hourly flux measurement following Kljun et al. (2004) to remove NEP values outside the forest boundary. Data

quality control, u_* threshold velocity and footprint filtering removed approximately 10.2% of the measured NEP data.

The partitioning of NEP into GEP and RE was achieved following procedures summarized below following Peichl et al. (2010) and Arain et al. (2022). RE was assumed to be equal to NEP at nighttime. The nighttime values of RE above the threshold were then used to model RE as a function of Ts and θ_{0-30cm}:

$$\mathrm{RE} = R_{10} \times Q_{10}^{\frac{Ts-10}{10}} \times \frac{1}{[1+\exp(a_1 - a_2\,\theta_{0-30cm})]} \qquad (1)$$

where a_1 and a_2 are empirically fitted parameters, with R_{10} and Q_{10} being fitted temperature response parameters, describing the relationship between RE and Ts. The modelled RE was used to gap-fill missing nighttime RE and estimate daytime RE. GEP was calculated by adding measured NEP to modelled daytime RE, with the gaps in GEP data being filled by the function:

$$\mathrm{GEP} = \frac{\alpha PARd\ A_{max}}{PARd + A_{max}} \times f(T_s) \times f(VPD) \times f(\theta_{0-30cm}) \qquad (2)$$

The first term describes the functional relationship between GEP and PAR, and the remaining terms define the response of GEP to VPD and θ_{0-30cm}.

The Rs measurements were processed and quality controlled using the SoilFluxPro Software (v4.2.1, LI-COR Inc.). Rs values associated with improperly closed and faulty soil CO_2 chambers were removed from the dataset. Start time analysis was carried out to optimize dead band times that did not fit the correct window in the measurement curve.

The Gaussian-gamma model following Khomik et al. (2009) was used to estimate Rs as a function of soil temperature (Ts), and soil moisture (θ) at 5cm depth:

$$\mathrm{Rs} = e^{(\beta_0 + \beta_{11}Ts + \beta_{12}Ts^2 + \beta_{21}\theta + \beta_{22}\ln(\theta))} \quad (3)$$

Where β_0, β_{11}, and β_{12}, β_{21}, and β_{22} are the model coefficients that are estimated in the regression analysis. 52% of the final soil chamber data were gap-filled using equation (3).

2.6. Data analysis

Temperature and precipitation anomalies were calculated by subtracting the flux station's observed monthly values from the 30-year (1981-2010) climate average (Environment Canada Weather Station at Delhi, Ontario). The corresponding weather station data record estimated the 90th percentile of the daily maximum temperature (T_{max}) to be 27.5°C for the 30-year climate average prior to the start of the study period (1971-2000). The threshold value of $T_{max} \geq 27.5$°C was used to identify "hot days", with years exhibiting 30 or more hot days being considered "hot years", following Arain et al. (2022).

Relative Extractable Water (REW) is a measure of the amount of soil water content available for plant extraction. REW was calculated using the equation:

$$\mathrm{REW} = \frac{\theta_{0-30cm} - \theta_{wp}}{\theta_{fc} - \theta_{wp}} \quad (4)$$

Where θ_{0-30cm} is the average soil water content for the top 30 cm of soil, θ_{wp} is the soil water content at wilting point, and θ_{fc} is the soil water content at field capacity. Site-

specific values for θ_{wp} and θ_{fc} were estimated to be 0.01 m^3 m^{-3} and 0.2 m^3 m^{-3}, respectively (Arain et al., 2022). Daily and annual drought analyses were conducted using REW calculations. Daily REW averages of ≤ 0.4 indicate "dry days" with years containing more than 62 consecutive dry days being considered "dry years" (Arain et al., 2022). Based on the climate and seasonality of the region, the growing season was determined to be between the calendar months of April to October. Winter season includes the months of December (from previous year) to March, spring contains April and May, summer contains June to September, and autumn comprises October and November.

A multivariate regression analysis was conducted using downward PAR, Ta, VPD, and θ_{0-30cm} as explanatory variables against non-gap-filled C fluxes of the forest at half-hourly and daily time scales, with the dataset limited to the daytime and the growing season. A residual analysis (Beamesderfer et al., 2020; Lindeman et al., 1980) was carried out to quantify the most significant explanatory variables influencing variability on GEP, RE and NEP.

In order to analyze the impacts of extreme weather events on forest productivity, the anomaly of C fluxes was calculated by subtracting daily sums of GEP, RE and NEP during extreme weather events from their corresponding non-extreme reference periods. Days of extreme weather for heat (T_{max} ≥ 27.5°C) and drought (REW ≤ 0.4) stress were identified and categorized. Reference periods were then calculated by averaging identical

non-extreme days of the year (DOY) over the study period. A two-sample t-test (table 4) was then conducted to determine the significance of the difference in means between identified extreme weather days and their respective non-extreme days. All calculations, analysis and processing were conducted using the MATLAB software (The MathWorks Inc.).

CHAPTER 3: RESULTS

3.1. Climate variability

Monthly mean downward PAR exhibited a similar pattern every year throughout the 14-year study period, reaching its peak values in June (Fig. 1a). The highest mean monthly PAR for the study period was recorded in 2020 (656 μmol m^{-2} $month^{-1}$), which was higher than the mean monthly PAR value of 567 μmol m^{-2} $month^{-1}$ in June. The most significant decline in mean monthly PAR was observed in 2015 and 2008, with the mean monthly PAR of 494 μmol m^{-2} $month^{-1}$ and 503 μmol m^{-2} $month^{-1}$, respectively, observed in June. The highest mean annual PAR value of 356 μmol m^{-2} yr^{-1} was observed in 2016, and the lowest was 311 μmol m^{-2} yr^{-1} in 2011. Year-to-year patterns of VPD followed Ta closely, reaching their peak values in July (Fig. 1a). The highest monthly mean VPD was recorded in July 2011 (0.93 kPa), coinciding with the highest recorded monthly mean Ta (23.8 ^{o}C). A high monthly VPD value (0.91 kPa) was also observed in June 2016 due to above-average downward PAR. 2021 recorded the lowest monthly mean PAR for July (481 μmol m^{-2} $month^{-1}$) and October (189 μmol m^{-2}

month^{-1}), coinciding with the lowest monthly VPD values of 0.43 kPa and 0.15 kPa for the two months, respectively.

The 14-year mean annual Ta (9.1 °C) indicates warmer conditions over the study period compared to the 30-year climate average (8.0 °C). Figure 1b displays monthly mean soil and atmospheric temperatures. The hottest year was 2012 (10.5 °C) with an exceptionally warm winter and the hottest mean March Ta (7.2 °C), compared to the 30-year climate average of 0 °C, resulting in an early start of the growing season. 2016 was another hot year with above-average winter temperatures and the hottest mean August Ta (23.2 °C). Furthermore, 2016 recorded the warmest summer, autumn and winter temperatures (Table 2). The 2021 study year recorded the highest monthly Ta for the months of June (20.4 °C), August (22.6 °C), and October (13.7 °C). The coldest year was 2014, with a mean annual Ta value of 7.5 °C and low temperatures persisting throughout the year, specifically in January (monthly mean Ta -8.0 °C) and March (monthly mean Ta -3.8 °C). 2019 was another cold year with below-average temperatures persisting until July. Fluctuations in soil temperature (Ts) correlate highly with variability in Ta measurements (R^2 = 0.96). The site experienced heat events in 2010, 2011, 2012, 2016 and 2018.

The 14-year mean total annual PPT was 1119 mm compared to the mean total annual PPT of 1036 mm for the 30-year climate average, indicating slightly wetter conditions during the study period. Annual PPT was highest in 2018 (1644 mm), with all seasons receiving ample precipitation (Table 2). During the period of August to November 2018, total PPT was 312 mm higher than the 30-year mean total PPT value over the same

period (Figure 1d). Winter of 2014 was the wettest on record and received a total PPT of 726 mm compared to the 30-year mean PPT of 294 mm for the corresponding period. January 2014 was the wettest month on record, with a total monthly PPT of 336 mm (Figure 1c). The highest total July and October PPT was observed in 2021, with the two months receiving 184 mm and 210 mm of PPT, respectively. The driest year was 2016 (778 mm), with below-average PPT evident in all seasons. PPT was noticeably absent during the 2016 growing season, resulting in drought conditions with a PPT deficit of 240 mm compared to the 30-year mean value for the corresponding period. Total PPT for the summer of 2017 was the lowest on record (196 mm), with a clear absence of PPT for July. REW, a measure of soil moisture, followed the same general pattern in a year, with peak values observed in early spring (Figure 1e) due to snowmelt. REW begins a sharp decline following the start of the growing season due to increasing rates of photosynthesis and evapotranspiration. The forest experienced drought events in 2011, 2012, 2016 and 2017. The most prolonged drought events were during the 2016 and 2017 study periods, with 127 and 121 consecutive dry days recorded for each year's growing season, respectively. Further, our observations demonstrated no significant change in meteorological variables in the post-thinning year.

3.2. Carbon flux dynamics

Figure 2 illustrates the time series of weekly total GEP, RE, and NEP values from 2008 to 2021. GEP reached its maximum by mid-July and then began to decline until the end of the growing season in October, after which the site became a net C source for the

winter season. The maximum weekly total GEP of 92 g C m^{-2} $week^{-1}$ was observed in 2015 and 2020, with the two years also having the highest total annual GEP for the study period (1895 g C m^{-2} and 1833 C m^{-2}, respectively). The site experienced its largest single event of C loss (16.74 g C m^{-2}) in mid-July 2011 due to exceptionally high Ta and VPD conditions. Furthermore, the longest growing season C loss event occurred in late July 2012 due to high VPD and Ta, during which the site remained a net C source of 10.6 g C m^{-2} for the month. The growing season's start varied each year; the earliest and latest starts were observed in 2012 (DOY 68; March 8) and 2018 (DOY 102; April 12), respectively. The hottest mean March Ta (7.2 °C) was responsible for the early start of the growing season in 2012, while abnormally low Ta in March and April 2018 caused the delayed start of photosynthesis. The summer of 2016 recorded the lowest total GEP (985 g C m^{-2}), highest mean Ta (21.2 °C), and lowest total PPT (220 mm) over the study period. The highest total Autumn RE (171 g C m^{-2}) was observed in 2021 due to above-average Ta and PPT, causing the site to become a net C source for seven consecutive days.

Figure 3 shows cumulative NEP for each year over the study period, offering insight into the inter-annual variability of the forest's carbon exchanges. Annual NEP ranged from 242 g C m^{-2} yr^{-1} in 2008 to 823 g C m^{-2} yr^{-1} in 2015. All years displayed a gradual decrease in NEP until the start of the growing season due to the prevalence of RE and the absence of GEP over the winter season. All years also followed a very close pattern in NEP until mid-March, after which they began to diverge due to the start of the growing

season. Despite a late start of the growing season (DOY 92; April 2), 2015 had the highest observed annual NEP (823 g C m^{-2} yr^{-1}) due to a noticeably productive summer when no usual decline or dip in NEP values was observed over the late summer. The highest total annual and summer GEP was also observed in 2015 due to moderate meteorological conditions during the year (Table 2). In the successive years of 2019 and 2020, we observed high productivity with annual NEP of 805 and 801 g C m^{-2} yr^{-1}, respectively, although each is driven by distinct factors. Lowest recorded annual RE (906 g C m^{-2} yr^{-1}) due to a cold growing season was responsible for the high net C uptake in 2019, while 2020 recorded the second-highest annual GEP (1833 g C m^{-2} yr^{-1}) over the study period due to moderate climate conditions. In contrast, during 2008, 2009, 2010, 2011, 2012, 2016 and 2018, NEP values showed a declining or slowing trend in the middle of the growing season due to extreme climate conditions as described earlier. This decline in NEP in the summer of extreme years caused their annual NEP values to decline to 242, 427, 511, 448, 490, 592 and 503 g C m^{-2} yr^{-1}, respectively, which was lower than or equal to the 14-year mean annual NEP value of 592 ± 169 g C m^{-2} yr^{-1} over the study period. For comparison, the mean annual NEP value of TP39 over the 14-year study period was 228 ± 92 g C m^{-2} yr^{-1}. It shows that on average, C sequestration at the TP74 was 2.6 times the C uptake at the older TP39 plantation. Moreover, despite experiencing a prolonged drought event in 2017, the site recorded NEP of 614 g C m^{-2} yr^{-1}, which is higher than the 14-year annual average. Explicitly, we observed GEP of 1644 g C m^{-2} yr^{-1} and RE of 1049 g C m^{-2} yr^{-1} for the same year.

The combined effects of heat and drought stress in 2011, 2012 and 2016 reduced annual GEP values to 1566, 1672 and 1639 g C m^{-2} yr^{-1}, respectively. Concurrently, we observed a moderate increase in RE with annual values of 1132, 1198 and 1058 g C m^{-2} yr^{-1}, respectively. In years with below-average temperatures and wet conditions during the growing season (2014 and 2019), we observed significant reduction in RE, resulting in higher net carbon uptake (Figure 4). In 2010 and 2018, annual RE saw a notable increase due to extreme heat and adequate soil moisture, reaching 1237 and 1124 g C m^{-2} yr^{-1}, respectively. Our observations indicate an upward trend in GEP with increasing plantation age, resulting in higher photosynthetic ability, while RE shows a decreasing trend with the older plantation (Figure 4a and 4b). During our study period, the combined effects of changing trends in GEP and RE with the aging plantation led to a pronounced growth in NEP. In Figure 4c, the linear regression line (slope = 28.6, $R^2 = 0.46$, $p < 0.05$) indicates a statistically significant positive relationship between NEP and forest age, while climate conditions influenced variability in individual years. Further, daily averages of Rs were measured and analyzed to explore the contribution of soil respiration (Rs) to overall RE (Figure 7). Rs accounted for approximately 89% of the total RE emitted (Figure 8), suggesting Rs is an integral and dominant part of the carbon flux in the forest ecosystem.

3.3. Disturbance impact on carbon flux

Thinning did not cause a large decrease in annual NEP value in our forest. In 2021, annual NEP was 648 g C m^{-2} yr^{-1}, which was slightly lower than the mean NEP value of

663 g C m^{-2} yr^{-1} over the 5-year pre-thinning period from 2016-2020. The mean annual NEP was 591 g C m^{-2} yr^{-1} from 2008-2021, which included thinning year. We also observed very high C sequestration at our nearby older TP39 forest site, where the annual NEP in 2021 was 373 g C m^{-2} yr^{-1}, which was much higher compared to the 14-year mean annual NEP value of 227 g C m^{-2} yr^{-1}. It shows that overall, 2021 was a very productive year for C sequestration in both plantation forests. However, despite experiencing ideal climate conditions in the first post-thinning year, annual GEP recorded in 2021 was lower than what our linear regression analysis anticipated (Figure 4a). Additionally, RE was higher than anticipated, as it exceeded the values predicted by the linear regression analysis (Figure 4b). We did not observe any appreciable change or anomaly in GEP and RE after thinning which deviates from normal inter-annual variability.

3.4. Environmental controls on carbon fluxes

The impact of extreme weather events on the C fluxes of our site over the study period is shown in Figure 5. High-temperature (T_{max}) conditions positively impacted photosynthesis rates leading to high GEP. Drought stress (REW_{min}) had a notable negative impact on GEP and caused reduced productivity due to water stress. The combined effects of heat and drought stress (T_{max} + REW_{min}) caused the most significant reduction in GEP. Like GEP, heat stress also had a positive impact on RE. Dry periods caused a reduction in RE due to a decline in soil moisture and, consequently, the reduction of soil microbial activity. The reduction in RE may also be attributed to

reduced GEP and related plant growth respiratory processes. Heat stress alone had a minor negative impact on NEP due to increased RE outweighing the growth of GEP, although, the reduction does not seem to be statistically significant (Table 4). Drought stress did not have any remarkable impact on NEP as the reduction of both GEP and RE offset the impact of each other (Table 4; Figure 5). Expectedly, combined drought and heat stress caused the most significant reduction in NEP due to diminished photosynthetic capability and enhanced RE as observed during peak growing season in some of the years such as in 2011, 2012 and 2016 (Figure 3).

Functional relationships among important meteorological variables (e.g. PAR, Ta, VPD, θ_{0-30cm}) and half-hourly day-time GEP, RE and NEP (non-gap-filled) fluxes for the growing season are illustrated in Figure 6. A rapid increase in GEP (Figure 6a) and NEP (Figure 6i) was evident with increasing PAR; however, the rapid rate of increase started to dissipate after PAR exceeded 1000 μmol m^{-2} s^{-1}. On average, the highest rates of GEP and NEP occurred near the PAR value of 1500 μmol m^{-2} s^{-1}, after which the rate started to decrease. The lack of a significant relationship between PAR and RE is apparent despite a slight surge in RE with increasing PAR in some years (Figure 6e). A continuous and rapid rate of increase was observed for GEP (Figure 6b) and NEP (Figure 6j) with increasing Ta until 15-20 °C, after which it started to plateau and eventually reversed. The rate of decline in productivity was just as intense as the rise of productivity, with lower GEP and NEP values observed at much higher temperatures.

Assessment of RE against Ta indicates an exponential increase in RE with rising Ta evident in all years (Figure 6f). Analysis of GEP (Figure 6c) and NEP (Figure 6k) against VPD indicates diminished productivity during exceptionally low VPD conditions (<0.1 kPa) caused by low light (PAR) conditions. Rates of photosynthesis grew rapidly with increasing VPD until about 0.9 to 1 kPa, after which it began to decline again with higher VPD, which indicates the high drying power of air, causing a reduction in stomatal opening and photosynthetic uptake. These observations also indicate a slight rise in RE at higher VPD (Figure 6g), although this relationship has been nonexistent in some years. A steady decline in GEP (Figure 6d) and NEP (Figure 6l) was evident with increasing θ_{0-30cm}, while the most optimal range for productivity was approximately values ranging from 0.07 to 0.08 m^3 m^{-3} for θ_{0-30cm}. Figure 6h displays an exponential decrease in RE with rising θ_{0-30cm}.

Multivariate regression analysis showed the relative impact of meteorological variables on carbon fluxes in the growing season (Table 3), where the relative contribution of explanatory variables (PAR, Ts, VPD, and θ_{0-30cm}) to the model was calculated by comparing the R^2 of the complete model to the R^2 of the partial model with a missing variable. Diurnal cycles had the strongest influence on GEP at half-hourly time scales, as PAR (radiation) accounted for 58% of the variability. Ts (temperature) and PAR had the greatest influence on daily GEP as they explained 38% and 19% of the variability, respectively. RE had the highest model R^2 for half-hourly and daily time scales (~ 0.8). Ts was the only variable with meaningful influence on RE and was able to explain 60%

of the variability at both time scales. Our study results showed that PAR and Ts were the primary explanatory variables for NEP at both half-hourly and daily time scales; however, the influence of PAR on NEP was less pronounced at a daily time scale. θ_{0-30cm} had a small positive impact on RE but lacked meaningful influence on GEP and NEP. VPD was also observed to influence GEP and NEP but to a smaller extent.

CHAPTER 4: DISCUSSION

4.1. Climate impact on carbon fluxes

Our study showed that PAR and Ta (Ts) are the primary variables driving productivity and growth in the forest ecosystem. Carbon sequestration rates during the growing season increased with rising Ta up to a threshold of ~23 °C, after which it started to decline. High Ta and VPD triggered diminished stomatal activity due to enhanced water loss, causing reduction in photosynthesis. For example, occurrence of exceptionally high Ta and VPD resulted in significant carbon loss during peak growing season in 2011, 2012 and 2016. We also found that high autumn Ta in combination with above-average precipitation could significantly reduce NEP due to large pulses of Rs and hence RE. Our study has indicated that soil moisture levels have significant impact on the plantation's carbon dynamics, in particular when coupled with extreme hot or cold conditions. Specifically, during periods of high soil moisture and low growing season temperatures, we observed a substantial reduction in RE, while GEP remained within the average rate (i.e. 2014 and 2019). Conversely, when soil moisture and temperature levels are both high, we observed a notable increase in RE (i.e., 2010 and 2018).

Ta had the strongest influence on carbon uptake rates in early spring as it regulates the start of the growing season. Years with substantially warm springs (i.e., 2010 and 2012) had the highest cumulative NEP from the start of the growing season until late May. The most crucial period during the growing season was from late May to mid-July, as the meteorological conditions during these peak summer months determined the trajectory of net carbon uptake for the remainder of the year. For instance, 2012 was the most productive year on record from mid-March to late May (Figure 3) while recording the hottest March and May mean Ta. However, the persistence of heat stress into the summer season, accompanied by high VPD and low soil water availability, caused 2012 to be one of the least productive years on record. Our findings agree with previous studies, which demonstrated although warmer spring temperatures promote early carbon uptake in forests of eastern North America, they lack significant impact on the annual productivity of the forest (Wu et al., 2012). Instead, the net carbon uptake is primarily determined by the meteorological conditions during late spring to mid-summer months (Beamesderfer et al., 2020; Dow et al., 2022). The trends of cumulative NEP in 2021 (Figure 3) for both TP74 and TP39 show how similar the two forests are in their response to climate conditions, as shown in their smaller peaks and troughs, particularly for the months of July, August, and October. The record high Ta and precipitation observed in October 2021, associated with a passing warm front caused a noticeable decline in cumulative NEP due to record high total October RE (124 g C m^{-2} $month^{-1}$) for the study period.

Dry conditions alone lacked a significant impact on the net carbon sink of the forest, with reductions observed in both GEP and RE offsetting each other. Our findings agree with previous studies that concluded that short-term and intense droughts cause higher losses of C from ecosystems than chronic droughts, with precipitation distribution expected to be a critical determinant influencing C losses from ecosystems (Frank et al., 2015; Hoover & Rogers, 2016). The increasing average global temperatures associated with climate change are projected to cause an increase in the severity, extent, and frequency of extreme weather (Peterson et al., 2014). Changing temperature and precipitation patterns can have various adverse impacts on forest C uptake that need to be further reviewed. For instance, a study conducted by Birch (1958) proved that rewetting soil following an extended period of drought with little or no precipitation results in powerful pulses of CO_2 being released into the atmosphere. We observed similar high Rs events in our soil CO_2 chamber data in late summer and fall, highlighting the significance of these episodic events on net C uptake in forests.

Heat and drought stress are two of the most important types of extreme weather that can significantly influence a forest's carbon dynamics. Our findings correspond to previous studies (Arain et al., 2022; von Buttlar et al., 2018) that recognized that the reduction in NEP associated with heat stress is caused by the dominant effect of Ts on RE outweighing growth in GEP. However, our results did not indicate a statistically significant reduction in NEP due to heat stress (Table 4; Figure 5). Coinciding hot and dry conditions can significantly reduce GEP by exacerbating soil moisture loss and

inhibiting transpiration and photosynthesis. Further, hot and dry conditions caused a minor increase in RE due to higher rates of soil microorganism activity (Rh and hence Rs). Years that experienced coinciding heat and drought stress (2011, 2012 and 2016) had reduced carbon sequestration capabilities, while years with moderate climate conditions exhibited the highest rates of productivity (i.e., 2015 and 2020).

4.2. Disturbance impact on carbon fluxes

Our study results showed that thinning did not significantly impact the forest's net C uptake in the first post-thinning year. Although, despite experiencing moderate climate conditions, carbon fluxes of the first post-thinning year were similar to that of years experiencing extreme heat and/or dry conditions (i.e., 2016 and 2017). However, the site remained a strong C sink with annual GEP, RE and NEP values within their interannual variability ranges. The impact of thinning on RE was less than we had anticipated considering the large amount of plant residue added to the forest floor when only logs were removed. Perhaps the slower decomposition rates in conifer needles and branches could explain it. We anticipate an increase in both GEP and RE in the upcoming years due to the availability of more light and water to remaining trees and the eventual decomposition of dead organic matter. It would be interesting to find out whether changes in GEP or RE dominate the net C uptake of the forest in post-thinning years. Similar findings were reported by Saunders et al. (2012), who did not find a significant impact of thinning on the NEP of a young spruce forest when comparing pre-thinning NEP to the two post-thinning years. However, a study conducted by Aun et al. (2021)

reported a reduction in NEP by 1.2 t C ha^{-1} yr^{-1} and 1.6 t C ha^{-1} yr^{-1} in young and middle-aged stands, respectively, two years after thinning.

Further investigation is warranted to fully understand the impacts of thinning on forest C uptake at our site since some processes operate on time scales longer than a year. The decomposition of dead organic matter of conifer trees is slow and can take up to a decade to fully take effect due to high lignin content (Prescott et al., 2005). Consequently, the impacts of thinning on RE and Rs will not be immediately apparent. Therefore, continuous observations in future are necessary to fully showcase the impact of thinning on C fluxes in this plantation stand.

4.3. Ecological and climatic implications

Abandoned agricultural lands in eastern North America have the large potential to support climate change mitigation and provide nature-based climate solutions through establishing plantation forests or natural re-growth forests. Reforestation or afforestation can result in not only providing a C sink but also stabilizing soil erosion, improving water quality and retention and improving the overall quality of the environment. The impact of forests and their management on water resources and water security is becoming very important in the face of climate change and increasing drought intensity and duration. Forest management practices such as thinning could not only help enhance C uptake but also help in the conservation and sustainability of forest water resources. Removal of weaker trees and maintaining low tree density through thinning also helps in improving

the health of the residual stands by increasing resource availability and reducing fire risks and insect mortality (Allen et al., 2010; Chmura et al., 2011). A meta-analysis conducted by Sohn et al. (2016) demonstrated that sites with moderate and heavy thinning had higher productivity during and after drought events compared to un-thinned stands.

Moreover, significant spatial heterogeneity has been observed in the climate, soil texture and species composition of forest ecosystems, highlighting the need for comparative studies in diverse regions. This would enable researchers to have a better understanding of the differences and similarities of forests and their response to extreme weather. Further, long-term observations provide valuable data for the training and validation of climate and ecosystem models. Through the incorporation of empirical data from different variables and ecosystems, modelers can improve the accuracy of models for simulating C uptake and predicting the response of forests to climate change. These models allow for improved policy-making, adaptation strategies and mitigation efforts with regard to climate change and extreme weather events.

CHAPTER 5: CONCLUSION

This study investigated the C flux dynamics of a young temperate pine plantation forest in Eastern North America using long-term eddy covariance flux data from 2008 to 2021 (14 years). We found that years exhibiting moderate climate conditions recorded the highest rates of productivity or NEP during the study period, while years that experienced coinciding heat and drought stress had the lowest rates of net C uptake. While the climate

of peak summer months determined the overall strength of the annual C sink, warm springs also had a noticeable influence on cumulative NEP, making the start of the growing season a critical period for the forest's net carbon uptake. Furthermore, high autumn temperatures accompanied by above-average precipitation significantly reduced C uptake due to large pulses of respiration. Our observations revealed cold and wet growing season conditions can enhance net carbon uptake by significantly reducing RE. We found that partial thinning or removal of about 1/3 of basal area in a highly productive young forest had no substantial impact on net C uptake in the first post-thinning year (2021) when compared to the 5-year pre-thinning mean annual NEP value. We anticipate an increasing trend in GEP and RE in this young forest over the post-thinning years. However, the eventual breakdown of dead organic matter left at site after the thinning may increase RE. At the same time, the promotion of photosynthetic capacity or GEP may also occur due to the availability of more light, water and nutrients to remaining trees or enhancement of the understory below the canopy following thinning. It would be interesting to observe which factor may dominate to influence the NEP of this stand in the coming years. The results from this study can be utilized to guide current and future management practices in plantation forests to enhance growth and C uptake productivity and to help in climate change mitigation.

REFERENCES

Allen, C. D., Macalady, A. K., Chenchouni, H., Bachelet, D., McDowell, N., Vennetier, M., Kitzberger, T., Rigling, A., Breshears, D. D., Hogg, E. H. (Ted), Gonzalez, P., Fensham, R., Zhang, Z., Castro, J., Demidova, N., Lim, J.-H., Allard, G., Running, S. W., Semerci, A., & Cobb, N. (2010). A global overview of drought and heat-induced tree mortality reveals emerging climate change risks for forests. *Forest Ecology and Management*, *259*(4), 660–684. https://doi.org/10.1016/j.foreco.2009.09.001

Arain, M. A., Xu, B., Brodeur, J. J., Khomik, M., Peichl, M., Beamesderfer, E., Restrepo-Couple, N., & Thorne, R. (2022). Heat and drought impact on carbon exchange in an age-sequence of temperate pine forests. *Ecological Processes*, *11*(1), 7. https://doi.org/10.1186/s13717-021-00349-7

Arain MA (2018a) AmeriFlux CA-TP3 Ontario—Turkey Point 1974 Plantation White Pine, Ver. 3–5, AmeriFlux AMP. https://doi.org/10.17190/AMF/12460 11.

Arain MA (2018b) AmeriFlux CA-TP4 Ontario—Turkey Point 1939 Plantation White Pine, Ver. 4–5, AmeriFlux AMP. https://doi.org/10.17190/AMF/12460 12.

Ashton, M. S., & Kelty, M. J. (2018). *The Practice of Silviculture: Applied Forest Ecology*. John Wiley & Sons.

Aun, K., Kukumägi, M., Varik, M., Becker, H., Aosaar, J., Uri, M., Buht, M., & Uri, V. (2021). Short-term effect of thinning on the carbon budget of young and middle-aged silver birch (Betula pendula Roth) stands. *Forest Ecology and Management*, *480*, 118660. https://doi.org/10.1016/j.foreco.2020.118660

Barr, A. G., Richardson, A. D., Hollinger, D. Y., Papale, D., Arain, M. A., Black, T. A., Bohrer, G., Dragoni, D., Fischer, M. L., Gu, L., Law, B. E., Margolis, H. A., McCaughey, J. H., Munger, J. W., Oechel, W., & Schaeffer, K. (2013). Use of

change-point detection for friction–velocity threshold evaluation in eddy-covariance studies. *Agricultural and Forest Meteorology*, *171–172*, 31–45. https://doi.org/10.1016/j.agrformet.2012.11.023

Beamesderfer, E. R., Arain, M. A., Khomik, M., & Brodeur, J. J. (2020). The Impact of Seasonal and Annual Climate Variations on the Carbon Uptake Capacity of a Deciduous Forest Within the Great Lakes Region of Canada. *Journal of Geophysical Research: Biogeosciences*, *125*(9). https://doi.org/10.1029/2019JG005389

Birch, H. F. (1958). The effect of soil drying on humus decomposition and nitrogen availability. *Plant and Soil*, *10*(1), 9–31. https://doi.org/10.1007/BF01343734

Bodo, A. V., & Arain, M. A. (2021). *Water Dynamics in the Understory of a Pine Plantation Forest After Variable Retention Harvesting* [Preprint]. In Review. https://doi.org/10.21203/rs.3.rs-1024732/v1

Brodeur, J. (2014). Data-driven approaches for sustainable operation and defensible results in a long-term, multi-site ecosystem flux measurement program. *McMaster University*, 249.

Chan, F. C. C., Altaf Arain, M., Khomik, M., Brodeur, J. J., Peichl, M., Restrepo-Coupe, N., Thorne, R., Beamesderfer, E., McKenzie, S., Xu, B., Croft, H., Pejam, M., Trant, J., Kula, M., & Skubel, R. (2018). Carbon, water and energy exchange dynamics of a young pine plantation forest during the initial fourteen years of growth. *Forest Ecology and Management*, *410*, 12–26. https://doi.org/10.1016/j.foreco.2017.12.024

Chmura, D. J., Anderson, P. D., Howe, G. T., Harrington, C. A., Halofsky, J. E., Peterson, D. L., Shaw, D. C., & Brad St.Clair, J. (2011). Forest responses to climate change in the northwestern United States: Ecophysiological foundations

for adaptive management. *Forest Ecology and Management*, *261*(7), 1121–1142. https://doi.org/10.1016/j.foreco.2010.12.040

Dow, C., Kim, A. Y., D'Orangeville, L., Gonzalez-Akre, E. B., Helcoski, R., Herrmann, V., Harley, G. L., Maxwell, J. T., McGregor, I. R., McShea, W. J., McMahon, S. M., Pederson, N., Tepley, A. J., & Anderson-Teixeira, K. J. (2022). Warm springs alter timing but not total growth of temperate deciduous trees. *Nature*, *608*(7923), 552–557. https://doi.org/10.1038/s41586-022-05092-3

Frank, D., Reichstein, M., Bahn, M., Thonicke, K., Frank, D., Mahecha, M. D., Smith, P., Velde, M., Vicca, S., Babst, F., Beer, C., Buchmann, N., Canadell, J. G., Ciais, P., Cramer, W., Ibrom, A., Miglietta, F., Poulter, B., Rammig, A., … Zscheischler, J. (2015). Effects of climate extremes on the terrestrial carbon cycle: Concepts, processes and potential future impacts. *Global Change Biology*, *21*(8), 2861–2880. https://doi.org/10.1111/gcb.12916

Healy, R. W., Striegl, R. G., Russell, T. F., Hutchinson, G. L., & Livingston, G. P. (1996). Numerical Evaluation of Static-Chamber Measurements of Soil—Atmosphere Gas Exchange: Identification of Physical Processes. *Soil Science Society of America Journal*, *60*(3), 740–747. https://doi.org/10.2136/sssaj1996.03615995006000030009x

Hoover, D. L., & Rogers, B. M. (2016). Not all droughts are created equal: The impacts of interannual drought pattern and magnitude on grassland carbon cycling. *Global Change Biology*, *22*(5), 1809–1820. https://doi.org/10.1111/gcb.13161

Khomik, M., Arain, M. A., Liaw, K.-L., & McCaughey, J. H. (2009). Debut of a flexible model for simulating soil respiration–soil temperature relationship: Gamma model. *Journal of Geophysical Research*, *114*(G3), G03004. https://doi.org/10.1029/2008JG000851

Kindermann, G., McCallum, I., Fritz, S., & Obersteiner, M. (2008). A global forest growing stock, biomass and carbon map based on FAO statistics. *Silva Fennica*, *42*(3). https://doi.org/10.14214/sf.244

Kljun, N., Calanca, P., Rotach, M. W., & Schmid, H. P. (2004). A Simple Parameterisation for Flux Footprint Predictions. *Boundary-Layer Meteorology*, *112*(3), 503–523. https://doi.org/10.1023/B:BOUN.0000030653.71031.96

Knapp, E. E., Bernal, A. A., Kane, J. M., Fettig, C. J., & North, M. P. (2021). Variable thinning and prescribed fire influence tree mortality and growth during and after a severe drought. *Forest Ecology and Management*, *479*, 118595. https://doi.org/10.1016/j.foreco.2020.118595

Lindeman, R. H., Merenda, P. F., & Gold, R. Z. (1980). *Introduction to bivariate and multivariate analysis*. Scott, Foresman. http://bvbr.bib-bvb.de:8991/F?func=service&doc_library=BVB01&local_base=BVB01&doc_number=001487319&line_number=0001&func_code=DB_RECORDS&service_type=MEDIA

Ostry, M. E., Laflamme, G., & Katovich, S. A. (2010). Silvicultural approaches for management of eastern white pine to minimize impacts of damaging agents: Silvicultural approaches for management of eastern white pine. *Forest Pathology*, *40*(3–4), 332–346. https://doi.org/10.1111/j.1439-0329.2010.00661.x

Papale, D., Reichstein, M., Aubinet, M., Canfora, E., Bernhofer, C., Kutsch, W., Longdoz, B., Rambal, S., Valentini, R., Vesala, T., & Yakir, D. (2006). Towards a standardized processing of Net Ecosystem Exchange measured with eddy covariance technique: Algorithms and uncertainty estimation. *Biogeosciences*, *3*(4), 571–583. https://doi.org/10.5194/bg-3-571-2006

Payn, T., Carnus, J.-M., Freer-Smith, P., Kimberley, M., Kollert, W., Liu, S., Orazio, C., Rodriguez, L., Silva, L. N., & Wingfield, M. J. (2015). Changes in planted forests

and future global implications. *Forest Ecology and Management*, *352*, 57–67. https://doi.org/10.1016/j.foreco.2015.06.021

Peichl, M., Arain, M. A., & Brodeur, J. J. (2010). Age effects on carbon fluxes in temperate pine forests. *Agricultural and Forest Meteorology*, *150*(7–8), 1090–1101. https://doi.org/10.1016/j.agrformet.2010.04.008

Peterson, D. L., Vose, J. M., & Patel-Weynand, T. (Eds.). (2014). *Climate Change and United States Forests* (Vol. 57). Springer Netherlands. https://doi.org/10.1007/978-94-007-7515-2

Prescott, C. E., Blevins, L. L., & Staley, C. (2005). Litter decomposition in British Columbia forests: Controlling factors and influences of forestry activities. *Journal of Ecosystems and Management*. https://doi.org/10.22230/jem.2005v5n2a298

Richart, M., & Hewitt, N. (2008). Forest remnants in the Long Point region, Southern Ontario: Tree species diversity and size structure. *Landscape and Urban Planning*, *86*(1), 25–37. https://doi.org/10.1016/j.landurbplan.2007.12.005

Saunders, M., Tobin, B., Black, K., Gioria, M., Nieuwenhuis, M., & Osborne, B. A. (2012). Thinning effects on the net ecosystem carbon exchange of a Sitka spruce forest are temperature-dependent. *Agricultural and Forest Meteorology*, *157*, 1–10. https://doi.org/10.1016/j.agrformet.2012.01.008

Skubel, R. A., Khomik, M., Brodeur, J. J., Thorne, R., & Arain, M. A. (2017). Short-term selective thinning effects on hydraulic functionality of a temperate pine forest in eastern Canada. *Ecohydrology*, *10*(1), e1780. https://doi.org/10.1002/eco.1780

Sohn, J. A., Saha, S., & Bauhus, J. (2016). Potential of forest thinning to mitigate drought stress: A meta-analysis. *Forest Ecology and Management*, *380*, 261–273. https://doi.org/10.1016/j.foreco.2016.07.046

von Buttlar, J., Zscheischler, J., Rammig, A., Sippel, S., Reichstein, M., Knohl, A., Jung, M., Menzer, O., Arain, M. A., Buchmann, N., Cescatti, A., Gianelle, D., Kiely, G., Law, B. E., Magliulo, V., Margolis, H., McCaughey, H., Merbold, L., Migliavacca, M., … Mahecha, M. D. (2018). Impacts of droughts and extreme-temperature events on gross primary production and ecosystem respiration: A systematic assessment across ecosystems and climate zones. *Biogeosciences*, *15*(5), 1293–1318. https://doi.org/10.5194/bg-15-1293-2018

Wilson, D. S., & Puettmann, K. J. (2007). Density management and biodiversity in young Douglas-fir forests: Challenges of managing across scales. *Forest Ecology and Management*, *246*(1), 123–134. https://doi.org/10.1016/j.foreco.2007.03.052

Wu, C., Gonsamo, A., Chen, J. M., Kurz, W. A., Price, D. T., Lafleur, P. M., Jassal, R. S., Dragoni, D., Bohrer, G., Gough, C. M., Verma, S. B., Suyker, A. E., & Munger, J. W. (2012). Interannual and spatial impacts of phenological transitions, growing season length, and spring and autumn temperatures on carbon sequestration: A North America flux data synthesis. *Global and Planetary Change*, *92–93*, 179–190. https://doi.org/10.1016/j.gloplacha.2012.05.021

Xu, B., Arain, M. A., Black, T. A., Law, B. E., Pastorello, G. Z., & Chu, H. (2020). Seasonal variability of forest sensitivity to heat and drought stresses: A synthesis based on carbon fluxes from North American forest ecosystems. *Global Change Biology*, *26*(2), 901–918. https://doi.org/10.1111/gcb.14843

TABLES

Table 1. Site characteristics

Site Characteristic	Condition
Tower location	42.707364°N 80.348524°W
Previous land use and management practices	Oak savanna prior to afforestation; stand thinned winter of 2021
Plantation year	1974
Elevation (m)	184
Dominant tree species	Pinus strobus
Water table depth (m)[b]	6-7
Basal area (m^2/ha)	35 (22)
Mean canopy height (m)[a]	16.2
Tree density (trees ha^{-1})[a]	1583
Leaf Area Index, LAI (m^2 m^{-2})[a]	6.6
Mean DBH (cm)[a]	17.90 (19.89)
Soil classification[a]	Brunisolic Gray Brown Luvisol
Soil water holding capacity[b]	Low to moderate
Soil texture[b]	~ 98% sand, 1% silt, <1% clay
Bulk density (g cm^{-3})[a]	1.376
Mineral soil carbon, 0-55 cm (t C ha^{-1})[c]	30.1
Mineral soil available P (ppm)[c]	117 ± 21
Mineral soil Mg (ppm)[c]	13 ± 6
Mineral soil K (ppm)[c]	10 ± 3
Mineral soil Ca (ppm)[c]	153 ± 107

Biometric measurements conducted in 2012. Values in brackets indicate post-thinning measurements (2021)

[a] Arain (2022)

[b] Peichl et al. (2010)

[c] Khomik et al. (2010)

Table 2. Annual and seasonal measurements of carbon fluxes and meteorological variables.

	Season	2008	2009	2010	2011	2012	2013	2014	2015	2016	2017	2018	2019	2020	2021
Total NEP ($g\ C\ m^{-2}$)	Winter	-55	-46	-33	-59	-23	-69	-67	-65	-32	-56	-61	-63	-55	-33
	Spring	131	147	190	149	205	172	187	235	205	221	129	185	208	199
	Summer	128	263	273	300	261	453	576	528	320	406	385	597	521	442
	Autumn	53	47	80	51	38	56	65	116	105	35	45	77	109	37
	Annual	**242**	**427**	**511**	**448**	**490**	**615**	**765**	**823**	**592**	**614**	**503**	**804**	**801**	**648**
Total GEP ($g\ C\ m^{-2}$)	Winter	0	16	34	4	91	16	6	8	71	33	10	14	38	49
	Spring	267	292	377	293	373	306	314	361	318	369	257	257	331	311
	Summer	1000	999	1128	1047	1017	1132	1168	1239	985	1034	1144	1173	1194	1084
	Autumn	161	155	187	187	194	205	205	260	264	194	179	179	196	205
	Annual	**1443**	**1485**	**1739**	**1566**	**1672**	**1668**	**1700**	**1895**	**1639**	**1644**	**1604**	**1692**	**1833**	**1666**
Total RE ($g\ C\ m^{-2}$)	Winter	90	70	76	75	127	98	80	82	125	106	86	88	108	94
	Spring	137	145	186	143	167	136	130	130	114	149	133	109	128	116
	Summer	873	735	855	747	756	680	594	713	664	628	760	578	675	646
	Autumn	108	108	108	143	136	152	131	144	159	160	136	122	133	171
	Annual	**1240**	**1066**	**1237**	**1132**	**1198**	**1068**	**949**	**1096**	**1058**	**1049**	**1124**	**907**	**1054**	**1039**
Mean Ta (°C)	Winter	-2.4	-3.0	-1.3	-3.7	1.8	-1.1	-5.5	-4.8	0.8	-0.5	-2.7	-2.3	0.2	-0.7
	Spring	10.1	10.8	12.6	10.0	12.1	10.4	9.9	11.5	9.7	10.9	9.8	9.4	8.8	10.7
	Summer	19.3	18.8	20.2	20.3	20.2	19.0	18.9	19.4	21.2	19.7	20.8	20.0	20.4	20.5
	Autumn	6.8	8.2	7.7	9.1	7.0	7.4	6.7	9.4	9.7	9.2	6.1	6.9	8.6	9.2
	Annual	**8.4**	**8.5**	**9.5**	**9.2**	**10.5**	**8.6**	**7.6**	**8.7**	**10.1**	**9.5**	**9.1**	**8.6**	**9.8**	**10.1**
Total PPT (mm)	Winter	317	428	221	362	318	376	726	143	290	357	590	404	353	240
	Spring	125	180	162	272	82	238	217	100	80	247	236	197	202	118
	Summer	347	336	347	289	415	409	327	317	220	196	573	318	388	433
	Autumn	130	135	181	264	179	199	251	175	118	257	326	196	143	273
	Annual	**1140**	**995**	**896**	**1293**	**1001**	**1266**	**1429**	**811**	**778**	**1153**	**1644**	**1128**	**1127**	**1009**
VPD (kPa)	Winter	0.11	0.11	0.14	0.09	0.16	0.11	0.09	0.09	0.14	0.11	0.10	0.10	0.11	0.15
	Spring	0.51	0.52	0.56	0.29	0.58	0.48	0.39	0.47	0.48	0.39	0.45	0.27	0.35	0.52
	Summer	0.60	0.49	0.53	0.60	0.68	0.45	0.49	0.50	0.71	0.58	0.53	0.54	0.62	0.51
	Autumn	0.25	0.23	0.25	0.26	0.21	0.22	0.21	0.28	0.23	0.27	0.16	0.20	0.26	0.17
	Annual	**0.36**	**0.33**	**0.35**	**0.32**	**0.41**	**0.30**	**0.29**	**0.32**	**0.40**	**0.34**	**0.31**	**0.29**	**0.35**	**0.34**
PAR ($\mu mol\ m^{-2}\ s^{-1}$)	Winter	163	189	185	179	175	160	189	193	171	172	199	183	178	193
	Spring	441	487	479	365	488	462	445	459	471	439	475	402	455	472
	Summer	470	471	481	485	499	480	492	487	549	520	518	509	536	483
	Autumn	208	177	207	179	172	183	166	222	224	200	161	195	181	172
	Annual	**319**	**332**	**337**	**311**	**334**	**322**	**329**	**338**	**356**	**339**	**343**	**332**	**341**	**333**

Table 3. Relative contribution of explanatory variables to the multivariate models of gross ecosystem productivity (GEP), ecosystem respiration (RE), and net ecosystem productivity (NEP). Models are estimated using non-gap-filled daytime growing season measurements at half-hourly and daily scales. NS indicates that the model variable was not significant.

	Daily			**Half-hourly**		
	GEP	**RE**	**NEP**	**GEP**	**RE**	**NEP**
PAR (% R^2)	18.69	NS	54.68	57.10	0.04	88.29
Ts (% R^2)	37.59	60.93	13.53	20.40	60.42	3.39
VPD (% R^2)	5.89	0.15	20.24	6.91	0.49	12.31
VWC (% R^2)	NS	3.95	0.72	NS	4.67	NS
Model R^2	0.70	0.79	0.36	0.63	0.78	0.47
F Statistic ($\alpha < 0.05$)	1.61E+03	2.63E+03	395	2.67E+04	5.33E+04	1.38E+04

Table 4. Results of two-sample two-tailed t-test assuming equal variance for the data samples of extreme days and their respective non-extreme reference days.

		Mean	SD	Variance	Sample Size	df	t-value	t-critical	p-value
GEP	Non-Extreme Heat Stress	9.51 10.64	1.97 1.54	3.87 2.39	68	134	3.72	1.98	0.00029
	Non-Extreme Drought	9.15 8.39	2.14 2.34	4.59 5.49	1050	2098	-7.75	1.96	1.39E-14
	Non-Extreme Heat + Drought	10.07 8.86	1.70 1.96	2.89 3.86	277	552	-7.74	1.96	4.77E-14
RE	Non-Extreme Heat Stress	5.67 7.05	1.62 1.96	2.63 3.85	68	134	4.47	1.98	1.64E-05
	Non-Extreme Drought	5.85 4.97	1.62 1.74	2.62 3.02	1050	2098	-12.02	1.96	3.06E-32
	Non-Extreme Heat + Drought	6.62 7.16	1.34 1.96	1.79 3.84	277	552	3.82	1.96	0.00015
NEP	Non-Extreme Heat Stress	3.86 3.62	1.80 2.09	3.24 4.37	68	134	-0.74	1.98	0.46
	Non-Extreme Drought	3.31 3.43	1.64 2.26	2.68 5.11	1050	2098	1.31	1.96	0.19
	Non-Extreme Heat + Drought	3.46 1.69	1.66 2.22	2.76 4.92	277	552	-10.64	1.96	3.40E-24

FIGURES

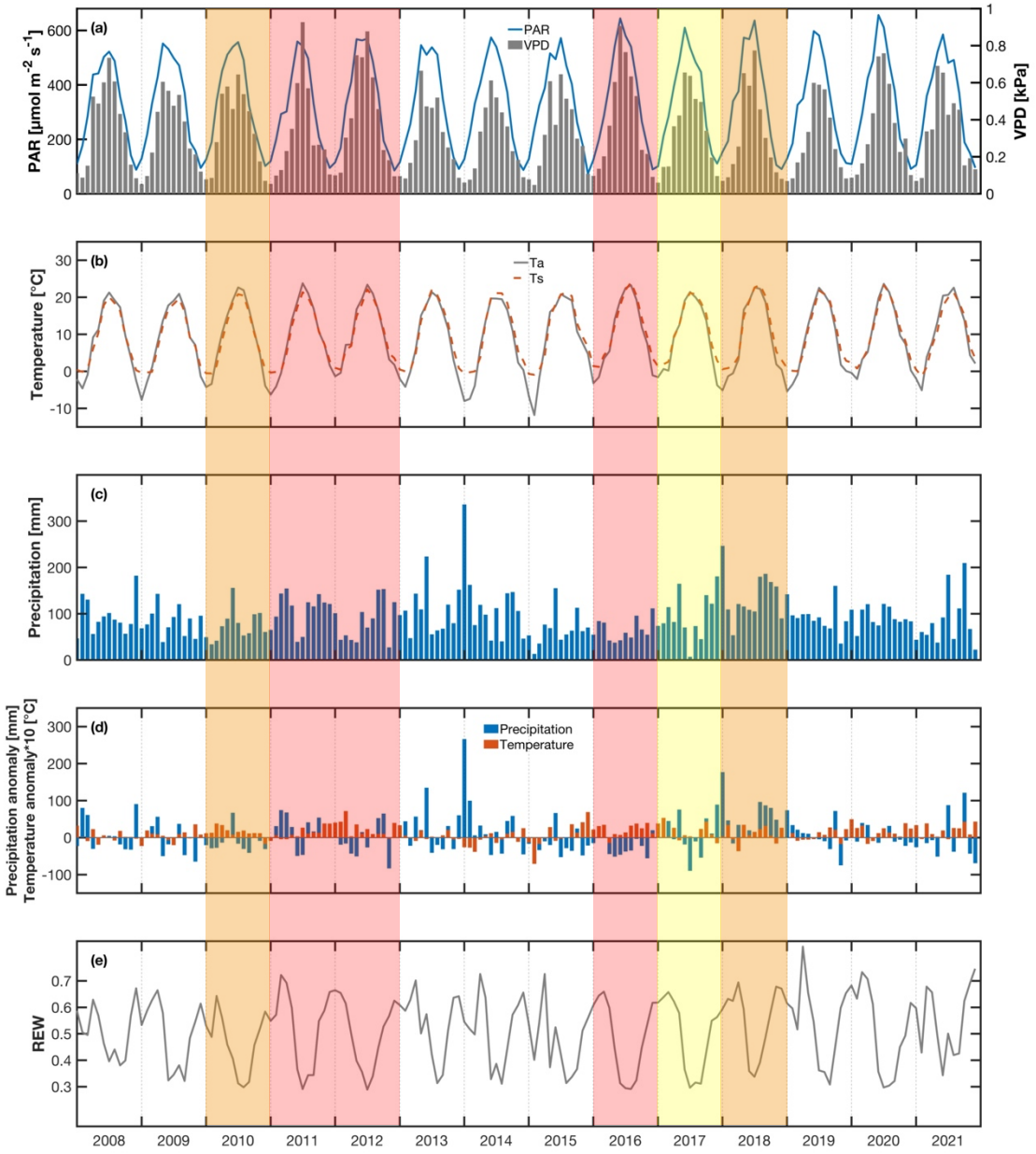

Figure 1. Monthly values of (a) mean photosynthetic active radiation (PAR) and vapour pressure deficit (VPD), (b) mean air temperature and soil temperature at 5cm depth, (c) total precipitation, (d) precipitation and temperature anomalies compared to the 30-year climate normal data (1981-2010) recorded at a weather station in Delhi, ON, and (e) mean Relative Extractable Water (REW) in the top 30cm of the soil. Hot years are shaded in orange, dry years shaded in yellow, and combined heat and drought years shaded in red.

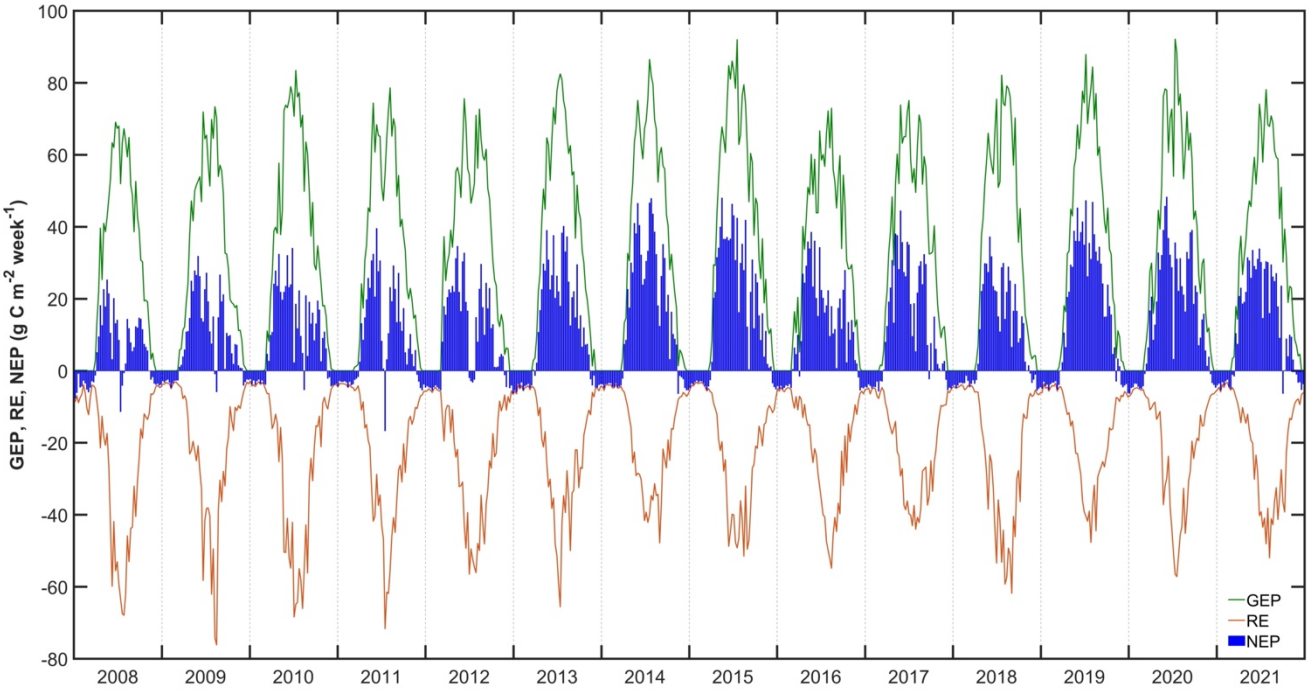

Figure 2. Weekly total gross ecosystem productivity (GEP), ecosystem respiration (RE), and net ecosystem productivity (NEP) for the study period.

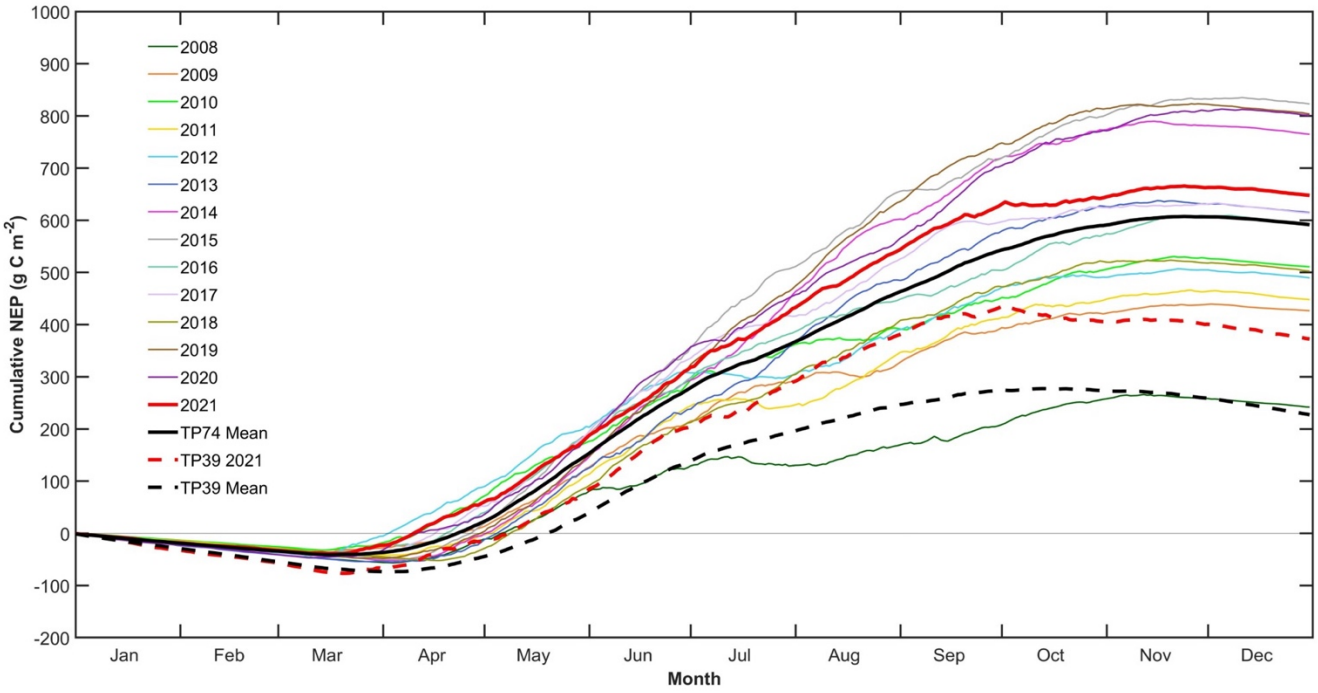

Figure 3. Cumulative annual net ecosystem productivity (NEP) for the study period.

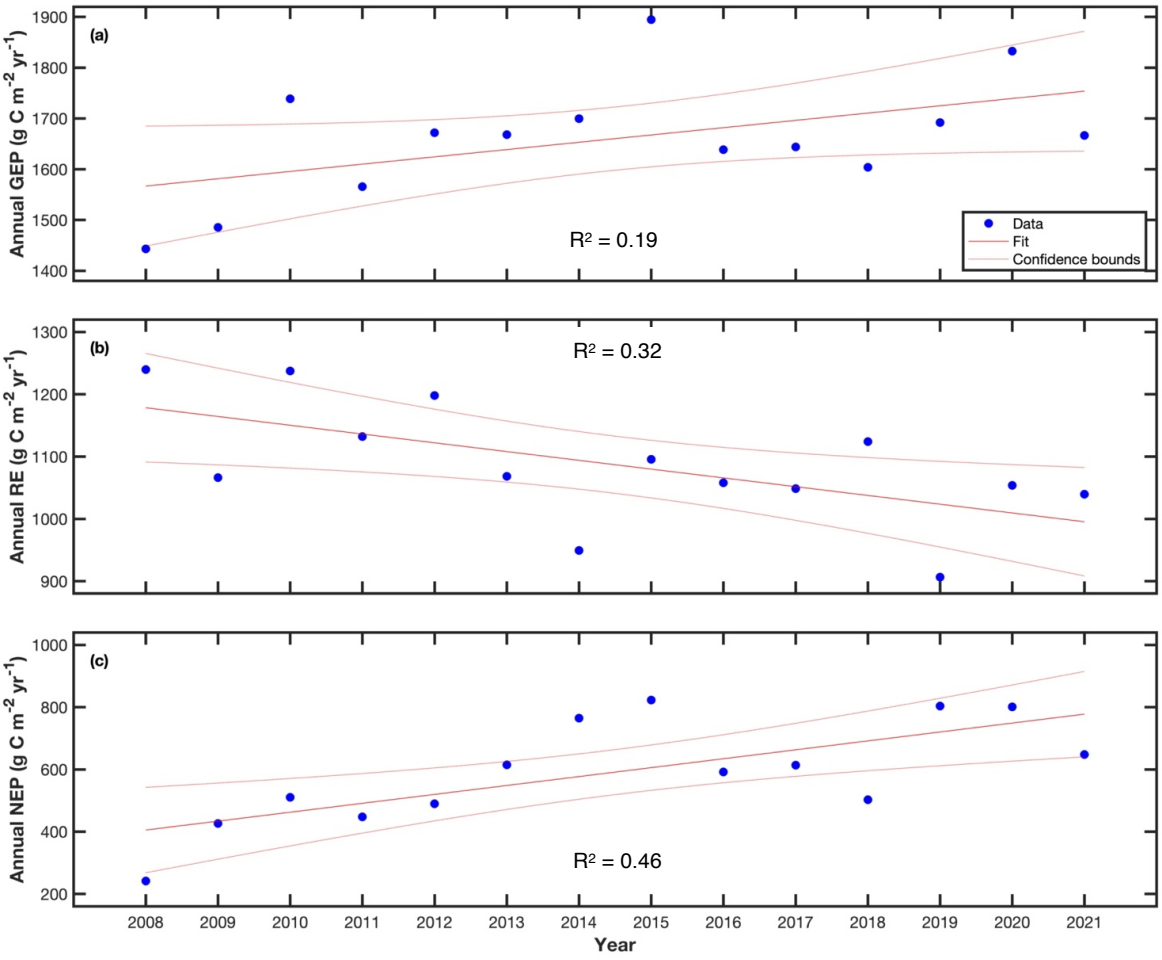

Figure 4. Correlation between forest age and total annual values of (a) gross ecosystem productivity (GEP), (b) ecosystem respiration (RE), and (c) net ecosystem productivity (NEP) during the study period.

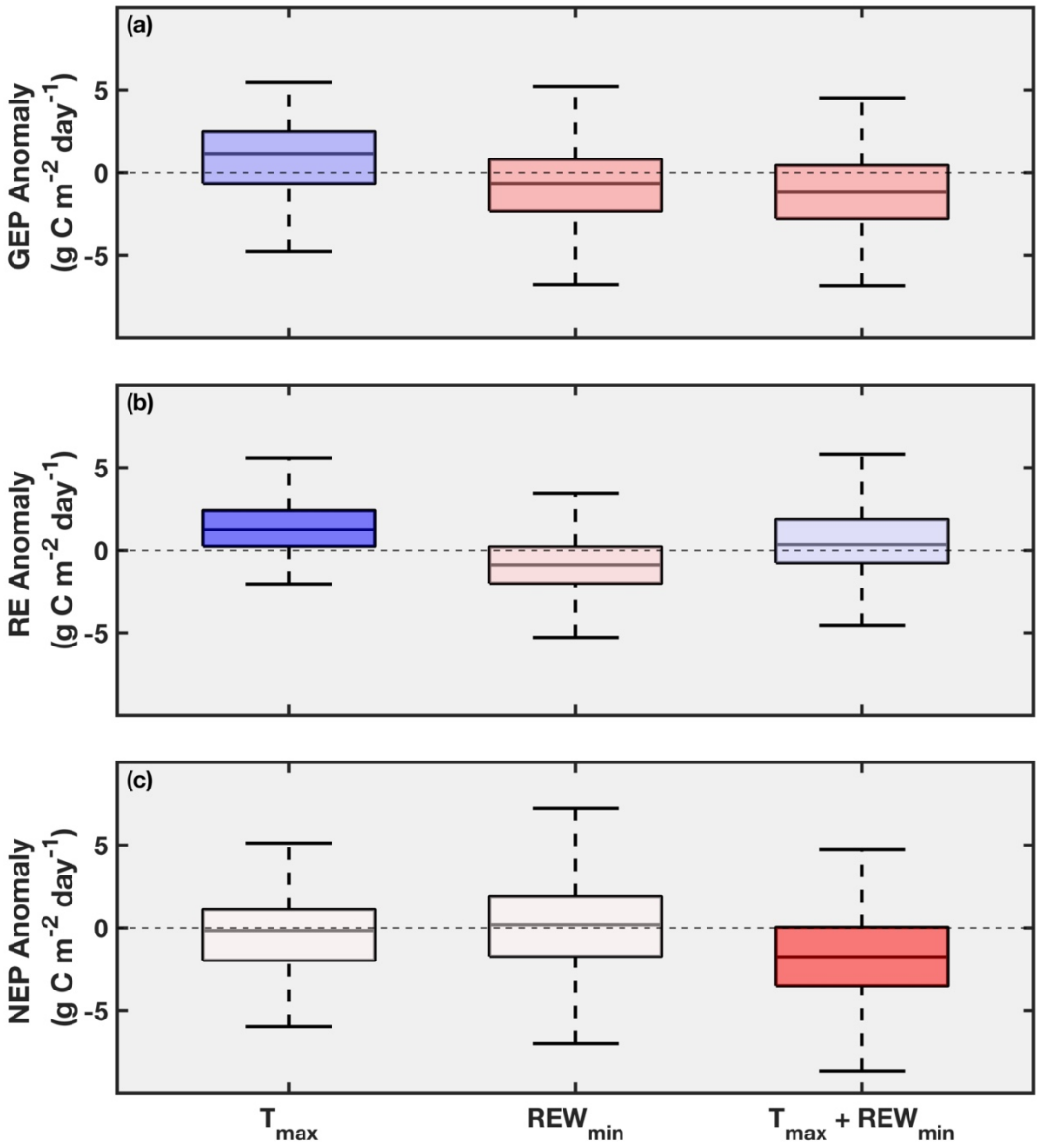

Figure 5. Impact of extreme events (drought (REW_{min}), heat-stress (T_{max}) and combined (REW_{min} + T_{max}) on (a) gross ecosystem productivity (GEP), (b) ecosystem respiration (RE), and (c) net ecosystem productivity (NEP) of the forest. Shown are differences between total daily carbon fluxes during days experiencing extreme weather and their respective non-extreme reference days (identical DOY) over the study period. Boxplots are colour coded based on mean anomaly (shade of red and blue for negative and positive anomaly, respectively).

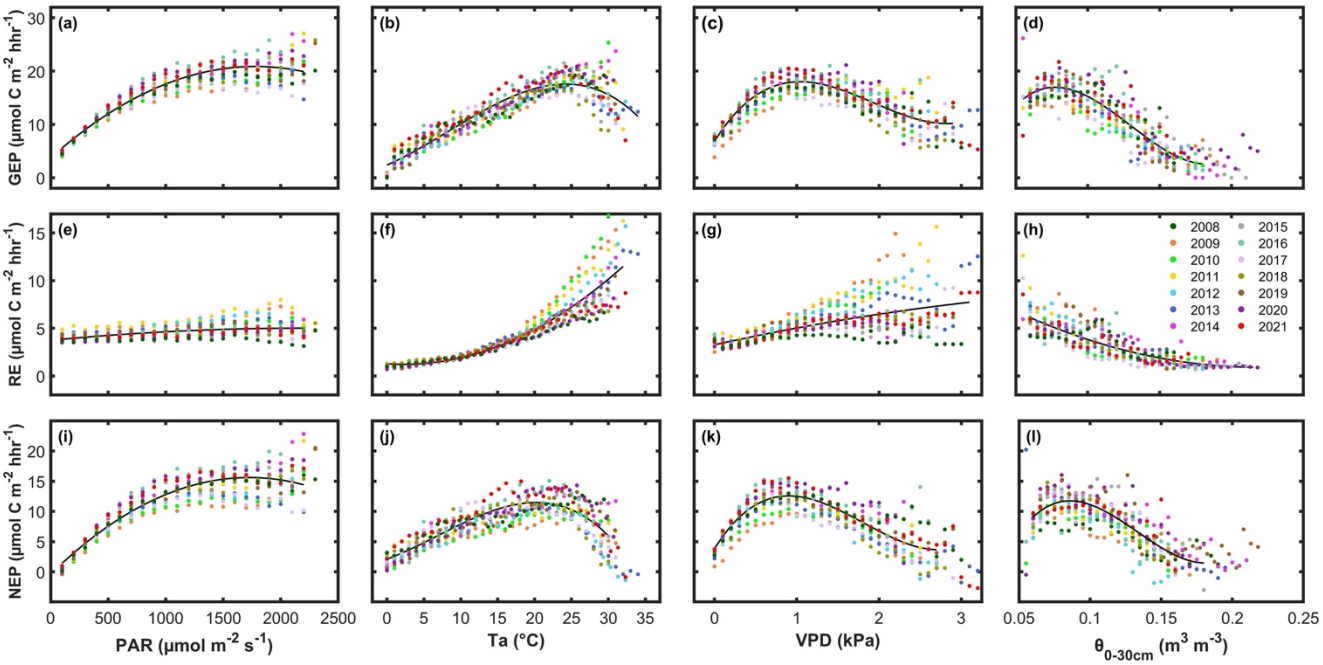

Figure 6. Correlation between daytime growing season measurements of (a) non-gap-filled gross ecosystem productivity (GEP) and bin-averaged photosynthetically active radiation (PAR, bin of 100 µmol m^{-2} s^{-1}), (b) bin-averaged air temperature above canopy (Ta, bin of 1°C), (c) bin-averaged vapour pressure deficit (VPD, bin of 0.1 kPa), and (d) bin-averaged volumetric water content ($\theta_{0\text{-}30cm}$, bin of 0.5%). Identical analysis applies to non-gap-filled (e-h) ecosystem respiration (RE), and (i-l) net ecosystem productivity (NEP). Solid black lines indicate the average fits.

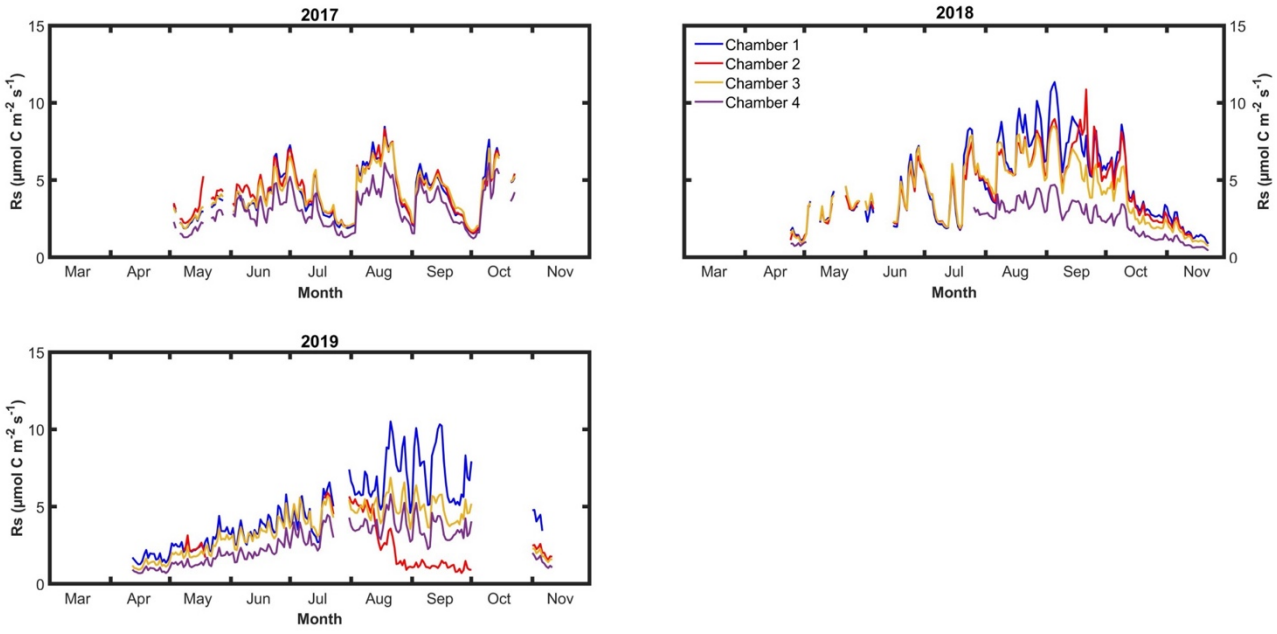

Figure 7. Daily average soil respiration (Rs) measurements using the LI-8100A automated soil CO_2 flux system. Missing 2020 and 2021 measurements due to lost data for most of the growing season.

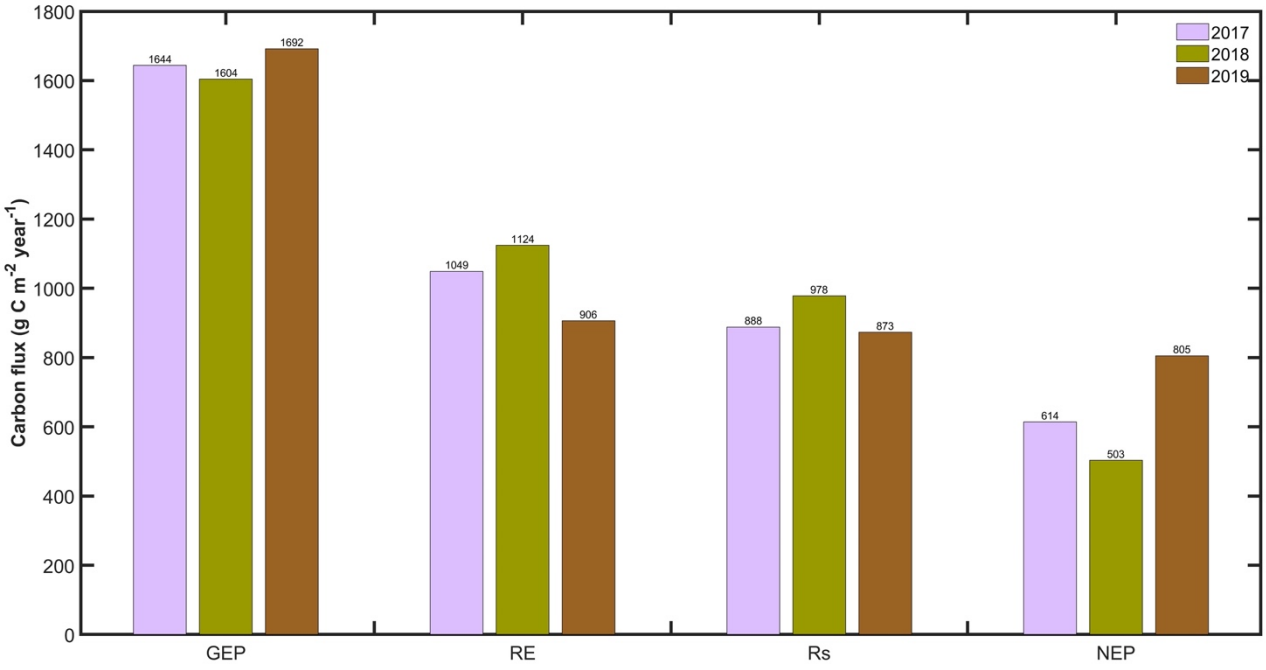

Figure 8. Annual values of gross ecosystem productivity (GEP), ecosystem respiration (RE) and net ecosystem productivity (NEP) from the eddy covariance system and soil respiration (Rs) measured using the automatic soil CO_2 chambers from 2017 to 2019.